Modulated reflectivity spectrum of strained $ZnSe/Zn_{1-x}Cd_xSe/ZnSe$ single quantum wells

R. G. Alonso, C. Parks, and A. K. Ramdas
Department of Physics, Purdue University, West Lafayette, Indiana 47907

H. Luo, N. Samarth, and J. K. Furdyna
Department of Physics, University of Notre Dame, Notre Dame, Indiana 46556

L. R. Ram-Mohan
Department of Physics, Worcester Polytechnic Institute, Worcester, Massachusetts 01609
(Received 3 September 1991)

The piezo- and electromodulated spectra of $ZnSe/Zn_{0.84}Cd_{0.16}Se/ZnSe$ single quantum wells, grown by molecular-beam epitaxy on (001) GaAs substrates, exhibit features associated with transitions between quantum confined levels. The transition energies are consistent with a theoretical model based on the $\mathbf{k}\cdot\mathbf{p}$ formalism and the transfer-matrix method. An unusually large ($\sim$40 meV) heavy-hole–light-hole splitting is observed in these quantum wells. The theoretical model accounts for the large splitting in terms of the strain arising from the lattice mismatch between the layers forming the quantum well. An excitonic model has been used successfully to account for the line shape of spectral features.

I. INTRODUCTION

The current intense interest in II-VI semiconductors (e.g., CdTe, HgTe, ZnS,. . .) and their heterostructures can be traced to the impressive range of energy gaps (zero for Hg-based II-VI compounds to 3.8 eV in ZnS) and the lattice constants which characterize them; these features are attractive from the point of view of basic physical issues and potential optoelectronic applications. Epilayers, quantum wells, and superlattices containing II-VI semiconductors have been successfully grown using molecular-beam epitaxy (MBE).[1] These include the subgroup of II-VI semiconductors in which a fraction of the group-II atoms are replaced by transition-metal ions such as Mn^{2+}, Co^{2+}, Fe^{2+},. . .; the magnetic properties of the layers of such diluted magnetic semiconductors introduce novel magnetic phenomena.[2,3] The promise, and in some instances, the successful realization of II-VI/III-V combinations offer further opportunities.[4]

We have previously studied Raman, photoluminescence, and modulated reflectivity spectra of MBE-grown $ZnSe/Zn_{1-x}Mn_xSe$ superlattices,[5,6] and $Cd_{1-x}Mn_xSe$ and $Zn_{1-x}Cd_xSe$ epilayers.[7,8] The single quantum wells studied in the present investigation contain ZnSe as the barriers and $Zn_{1-x}Cd_xSe$ as the well. In the bulk, $Zn_{1-x}Cd_xSe$ is expected to have the zinc-blende structure for low x and the wurtzite structure for high x. However, incorporated as an epilayer or in a superlattice grown on a (001) GaAs substrate, $Zn_{1-x}Cd_xSe$ exhibits the zinc-blende structure throughout the whole composition range.[1,7] The lattice parameter of this alloy varies linearly with x, which results in a lattice mismatch proportional to x in the $ZnSe/Zn_{1-x}Cd_xSe/ZnSe$ single quantum wells. These quantum wells are of excellent quality; in fact, $ZnSe/Zn_{1-x}Cd_xSe/ZnSe$ single quantum wells grown under similar conditions have been successfully used to fabricate an optically pumped blue laser.[9]

As has been extensively documented, modulated reflectivity is a powerful technique in the study of electronic transitions between quantum confined levels in quantum wells and superlattices. Piezomodulated and photomodulated reflectivity have been fruitfully exploited in the study of bulk semiconductors and their heterostructures.[10,11] Note that in some cases the photomodulated reflectivity signal—which effectively is contactless electromodulated reflectivity—is overwhelmed by a strong photoluminescence. While the piezomodulation technique does not suffer from this limitation, it is also feasible to perform an electromodulated reflectivity study free from photoluminescence by applying an electric field directly with a pair of electrodes.[12] Experience has shown that for each system under investigation the appropriate modulation technique has to be suitably selected.

In this paper we report a piezomodulated and electromodulated reflectivity study of the quantum confined electronic transitions in strained $ZnSe/Zn_{0.84}Cd_{0.16}Se/ZnSe$ single quantum wells of 60, 90, and 120 Å well widths, respectively.

II. EXPERIMENTAL PROCEDURE

The $ZnSe/Zn_{1-x}Cd_xSe/ZnSe$ quantum wells used in the present study were grown by molecular-beam epitaxy (MBE) on (001) GaAs substrates. The sample parameters are given in Table I. the sample quality and layer thickness are determined by low-angle x-ray diffraction and transmission electron microscopy. The growth direction is designated by $\hat{z}$ in this paper.

The piezomodulation of the reflectivity spectrum of the crystals is accomplished by mounting the sample on a lead-zirconate-titanate transducer driven by a sinusoidal

TABLE I. Parameters of the single quantum wells, l_w denoting the well width.

Sample	Well	Barrier	l_w (Å)
SQW-4	$Zn_{0.84}Cd_{0.16}Se$	ZnSe	60
SQW-5	$Zn_{0.84}Cd_{0.16}Se$	ZnSe	90
SQW-6	$Zn_{0.84}Cd_{0.16}Se$	ZnSe	120

electric field with the field along its thickness. The alternating expansion and contraction of the transducer subjects the sample to an alternating strain with a typical rms value of $\sim 10^{-5}$. We have also investigated the electromodulated reflectivity spectrum of the samples. The electromodulation technique[13] is accomplished by placing the thin samples between two copper electrodes. The modulation is provided by a 930-Hz alternating voltage of 560 V (rms) applied between the two electrodes. The breakdown electric field of He gas at 6 K limits the applied voltage to less than 600 V inside the cryostat environment. The sample is mounted directly on one electrode plate, while the other plate is placed about 1 mm in front of the sample surface. The "front" plate has a 1×8 mm^2 slit to allow the probe radiation to impinge on the sample and exit after reflection. This technique does not require any special sample preparation, and, in particular, no leads are attached directly to the sample.

A variable temperature stainless-steel cryostat[14] is employed for low-temperature measurements down to 6 K. A Perkin-Elmer (Model E-1) double-pass grating monochromator with a tungsten-halogen lamp as a source and an uv-enhanced Si photodiode constituted the spectrometer. The modulated part of the reflected radiation (ΔR) was detected and amplified with a phase-sensitive lock-in amplifier. The signal, after analog to digital conversion, was processed with a microcomputer.

The photoluminescence spectra are excited with monochromatic radiation from an Ar^+ laser. For low-temperature measurements, the power of the incident beam is typically kept below ~ 75 mW in order to avoid sample heating. Low-temperature measurements were again carried out using the variable-temperature optical cryostat. The photoluminescence radiation is spectrally analyzed with a computer-controlled double (triple) SPEX monochromator and detected with standard photon-counting electronics.

III. RESULTS AND DISCUSSION

A. Modulated reflectivity

In the piezomodulated reflectivity experiments, the normalized modulated reflectivity can be expressed by[15]

$$\frac{\Delta R}{R}=\alpha\,\Delta\epsilon_r+\beta\,\Delta\epsilon_i\ , \tag{1}$$

where α and β are the so-called Seraphin coefficients, and $\Delta\epsilon_r$ and $\Delta\epsilon_i$, respectively, are the change of the real and imaginary parts of the dielectric constants as a result of changing the energy gap of the sample due to stress. For a spectrum in the vicinity of an n-dimensional critical point, the change of the complex dielectric constant resulting from the stress modulation is given by[16]

$$\frac{d\epsilon(\omega)}{d\omega_g}=-i^{r-n}C_n(\omega-\omega_g+i\Gamma)^{(n/2)-2}\ , \tag{2}$$

where C_n is the spectral amplitude which is proportional to the square of the momentum matrix, $\hbar\omega$ is the photon energy, $\hbar\omega_g$ is the energy gap of the specimen, Γ is the Lorentzian broadening parameter, and r corresponds to the M_r critical point. For discrete excitons n is zero. In order to determine the energy position of the features accurately we have performed line-shape fittings for all the signatures associated with transitions between quantum confined levels.

Figure 1 shows the piezomodulated reflectivity spectrum of a $ZnSe/Zn_{0.84}Cd_{0.16}Se/ZnSe$ single-quantum-well structure with a well width of 90 Å. The spectrum was recorded at 6 K. The various signatures around 2.8 eV originate from the ZnSe barrier. The large feature at 2.81 eV is attributed to the excitonic transition in ZnSe, while the features at 2.82 and 2.825 eV remain unidentified. The remaining features below 2.8 eV we identify with the electronic transitions of the $Zn_{0.84}Cd_{0.16}Se$ single quantum well. We label them according to the initial mth heavy- (H) hole or mth light- (L) hole valence subband to the final nth conduction subband. Thus the energies of such intersubband transitions are given by

$$E_{n,m}=E_g+E_{n,e}+E_{m,h}-E^B_{n,m}\ , \tag{3}$$

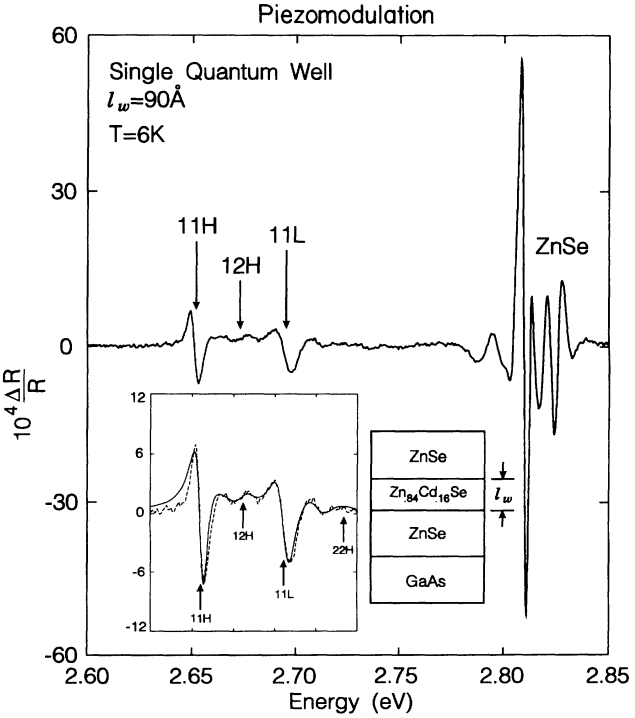

FIG. 1. Peizomodulated reflectivity spectrum of a $ZnSe/Zn_{0.84}Cd_{0.16}Se/ZnSe$ single-quantum-well structure with a well width of 90 Å. The spectrum was recorded at 6 K. Also shown in the inset of the figure is a theoretical line-shape fitting.

where E_g is the band gap of $Zn_{0.84}Cd_{0.16}Se$, $E_{n,e}$ is the energy of the nth subband of electrons, $E_{m,h}$ is the energy of the mth subband of holes, and $E^B_{n,m}$ is the binding energy of the exciton in the quantum-well structure with its two-dimensional characteristics. The signatures at 2.701 and 2.652 eV correspond to the $11H$ and $11L$ transitions, respectively, between quantum confined levels in the conduction and valence bands. The energies of the quantum confined transitions were determined from the theoretical line-shape fitting shown in the inset of Fig. 1.

The piezomodulated reflectivity spectra of the three $ZnSe/Zn_{0.84}Cd_{0.16}Se/ZnSe$ quantum wells studied in the present investigation are collectively shown in Fig. 2. The characteristics of these single quantum wells are listed in Table I. The spectra were obtained at $T=6$ K. The features shown are attributed to transitions between quantum confined levels and are labeled accordingly. Since the well and the barrier composition are the same in all three single quantum wells, the differences in the transition energies can be traced to the well widths, these being 60, 90, and 120 Å, respectively; the narrower the well, the higher the energy of a given transition. As expected, all three peaks are blueshifted from E_g(well)$=2.62$ eV, the energy gap of the well being calculated from the x dependence of the energy gap in zinc-blende $Zn_{1-x}Cd_xSe$.[7]

Electromodulated reflectivity as applied to bulk crystals has been described as a "third-derivative" technique.[17] However, when applied to quantum-well structures it yields a "first derivative,"[18] and hence similar line shapes of the piezomodulated and electromodulated reflectivity features in quantum wells. In the quantum wells investigated in the present work, the modulated reflectivity features appeared more distinct in the electromodulated spectra, described below, as compared to those in the piezomodulated spectra.

Figure 3 shows the electromodulated reflectivity spectrum of the 90-Å $ZnSe/Zn_{0.84}Cd_{0.16}Se/ZnSe$ quantum well. The series of sharp features near 2.8 eV once again corresponds to the ZnSe barrier. The $11H$, $11L$, and $22H$ transitions are clearly observed. The transition at 2.676 eV can be attributed to either the forbidden $12H$ transition or to the signature of the $2s$ exciton associated with the $11H$ transition. We note that the $12H$ forbidden transition can arise from the mixing of heavy-hole and light-hole bands.[19] On the other hand, if the 2.676-eV feature is attributed to the $2s$ exciton associated with the $11H$ transition, it implies an excitonic binding energy of 29 meV, close to the ~ 30 meV actually expected.[20] The large heavy-hole–light-hole splitting of ~ 40 meV is mainly due to the strain originating in the lattice mismatch. In the absence of strain our theoretical model predicts only a 4-meV heavy-hole–light-hole splitting, whereas in order to account for the splitting observed experimentally, the model requires a 0.62% strain in the well. We note here that the strain assumed is somewhat smaller than the 1% that would arise if only the well layer is strained to accommodate the lattice mismatch; presumably the smaller strain of the well layer is indicative of strain in the barriers also.

The electromodulated reflectivity spectra of the three $ZnSe/Zn_{0.84}Cd_{0.16}Se/ZnSe$ quantum wells studied in the

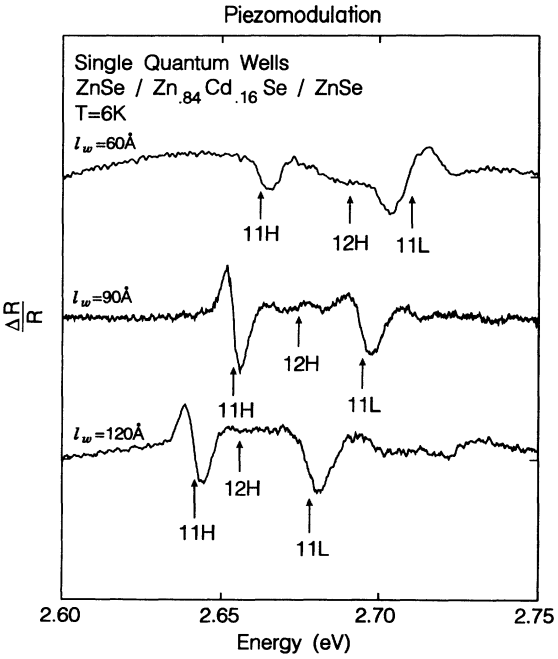

FIG. 2. Piezomodulated reflectivity spectra of three $ZnSe/Zn_{0.84}Cd_{0.16}Se/ZnSe$ quantum wells with well widths of 60, 90, and 120 Å, respectively, showing the signatures from the quantum-well confined transitions.

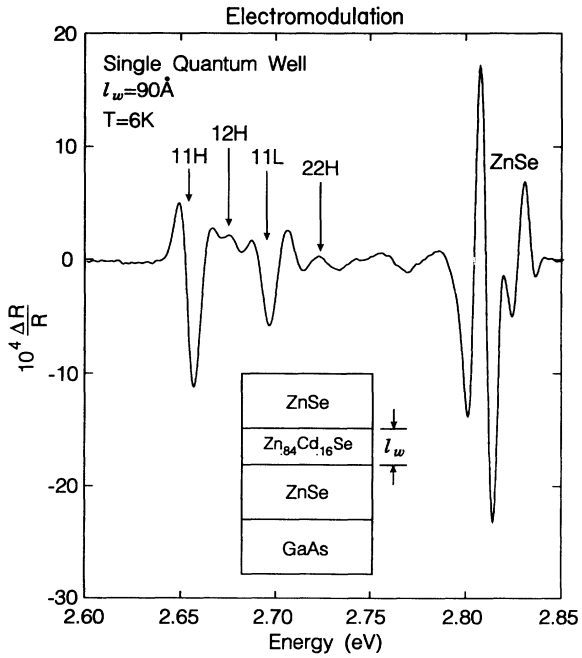

FIG. 3. Electromodulated reflectivity spectrum of a $ZnSe/Zn_{0.84}Cd_{0.16}Se/ZnSe$ single-quantum-well structure with a well width of 90 Å. The spectrum was recorded at 6 K.

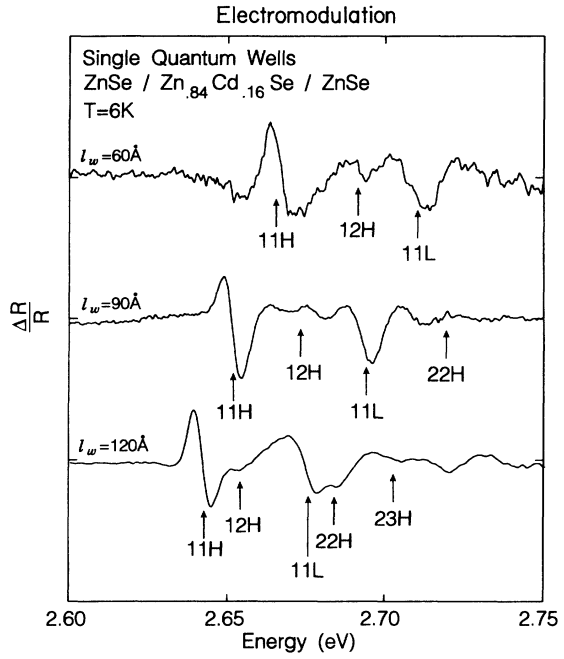

FIG. 4. Electromodulated reflectivity spectra of three $ZnSe/Zn_{0.84}Cd_{0.16}Se/ZnSe$ quantum wells with well widths of 60, 90, and 120 Å, respectively, showing the signatures from the quantum-well confined transitions.

present investigation are compared in Fig. 4, the spectra being obtained at $T=6$ K. The energies of the electromodulated reflectivity features match those observed in the piezomodulated reflectivity spectra.

B. Energy-level calculations

In order to confirm the identification of the modulated reflectivity signatures with optical transitions between quantum confined levels, we have carried out a series of energy-band calculations. Given the lattice mismatch between the barrier and the well, the theoretical model has to account for the effect of strain, which contributes to the heavy-hole–light-hole splitting of the valence band of the well, in addition to the splitting already present due to the reduced symmetry of the single quantum well. In these quantum wells the strain-induced splitting can be *one order of magnitude* larger than the splitting due to the reduced symmetry.

The energies of the confined levels in these single quantum wells have been calculated using an eight-band Kane model Hamiltonian for each layer and the transfer-matrix method.[21] The transfer-matrix method, originally applied to superlattices, can also be exploited to deduce the quantum confined states in the single quantum well. This is accomplished by considering a superlattice in the limit of a very large barrier width and by selecting solutions with the z component of the electronic $\mathbf{q}$ vector in the middle of the Brillouin zone.[22]

The Hamiltonian for a layer, either the well or the barrier, is given by

$$\mathcal{H}=-\frac{\hbar^2}{2m}\nabla^2+V(r)+\frac{1}{4m^2c^2}(\sigma\times\nabla)\cdot\mathbf{p}+\mathcal{H}_{\text{strain}} . \quad (4)$$

The matrix elements of the strain-free Hamiltonian are those given by Weiler.[23] The deformation-potential Hamiltonian is given by[24]

$$\mathcal{H}_{\text{strain}}=C_c\sum_i\varepsilon_{ii}-a_v\sum_i\varepsilon_{ii}-b_v\sum_i\varepsilon_{ii}(J_i^2-\tfrac{1}{3}J^2)$$
$$-\frac{d_v}{\sqrt{3}}\sum_{i<j}\varepsilon_{ij}\{J_iJ_j\} , \quad (5)$$

where C_c is the conduction-band deformation-potential constant, a_v is the valence-band hydrostatic deformation-potential constant, b_v and d_v are the shear deformation-potential constants, and ε_{ij} are the components of the strain tensor. This term has been introduced to account for strain in the quantum-well layer due to the lattice mismatch. In the present calculation the

TABLE II. Transition energies in eV at 6 K.

Sample (well width)	Transition	Reflectivity (eV)	Photoluminescence (eV)	Theory (eV)
SQW-4 (60 Å)	11*H*	2.664	2.659	2.662
	12*H*	2.691		2.695
	11*L*	2.710		2.710
SQW-5 (90 Å)	11*H*	2.654	2.648	2.654
	12*H*	2.676		2.673
	11*L*	2.695		2.695
	13*H*			2.699
	22*H*	2.722		2.722
SQW-6 (120 Å)	11*H*	2.641	2.634	2.641
	12*H*	2.653		2.652
	13*H*			2.670
	11*L*	2.675		2.677
	21*H*			2.675
	22*H*	2.685		2.687
	23*H*	2.700		2.705

strain along x in the well is considered to be an adjustable parameter although it can be estimated from the lattice mismatch, while the strain along z is derived from the strain-stress relations which give $\varepsilon_{zz} = -(2c_{12}/c_{11})\varepsilon_{xx}$. The input parameters used for the computation[21] are the energy gap E_g, the spin-orbit splitting of the valence band Δ, the interband matrix element **p**, the valence-band Luttinger parameters, the deformation potentials for each layer, the valence-band offset,[6,20] and the dimensional parameters of the superlattice.

The results of the theoretical calculation are presented in Table II and compared with the experimental results. As can be seen, the calculated values for the quantum-well transitions are in good agreement with the modulated reflectivity results. The theoretical calculation shows that the 60-Å strained quantum well has two confined electronic levels in the conduction band, and two heavy-hole levels and one light-hole level in the valence band. The presence of the second heavy hole ($2H$) as well as the absence of a third electronic level are the result of the strain. The 90-Å quantum well, being wider, contains more confined states: three electron states, three heavy-hole states, and one light-hole state. The 120-Å quantum well contains four electron states, three heavy-hole states, and one light-hole state; of these, the third heavy-hole ($3H$) state is confined due to strain. The comparison of the energies of the experimentally observed signatures with the calculated energy levels presented in Table II shows that in the 60-Å well only the electronic transitions from the hole levels to the first electronic level are observed, whereas for the wider wells transitions to the second electronic level have been also identified.

The photoluminescence spectra of these single quantum wells reproduce the experimental results previously reported in Figs. 1, 2, and 3 in Ref. 25, including the observation of a strong resonance enhanced Raman peak associated with the 2LO phonon of the $Zn_{0.84}Cd_{0.16}Se$ well. This Raman peak exhibits an intensity comparable to that of the photoluminescence due a close match between the energy of the Raman peak and that of the electronic transition underlying the luminescence and thus resulting in an "out-resonance."[26] Photoluminescence yields the transition energy between the lowest quantum confined states in agreement with the position of the $1H$ features in the modulated reflectivity spectra reported in this paper. The present work underscores the advantage of modulated reflectivity which allows one to observe transitions involving higher-lying confined states.

IV. CONCLUDING REMARKS

Optical studies in heterostructures containing alloys of wide-band-gap II-VI semiconductors offer the opportunity of observing transitions from quantum confined states with energies well into the blue region of the spectrum. The feasibility of laser action in the blue region has generated considerable interest in these heterostructures[9] and hence the characterization of the electronic parameters of $ZnSe/Zn_{1-x}Cd_xSe/ZnSe$ quantum-well structures is particularly important. In the present paper we have demonstrated that piezomodulated and electromodulated reflectivity provides valuable information on these quantum-well structures in view of the large number of electronic transitions which can be observed. The experimental access to a large number of quantum confined states in this technique allows a detailed comparison with the calculations; the present work in particular highlights the importance of strain in determining the energies of the confined states, as reflected in the pronounced heavy-hole–light-hole splitting.

ACKNOWLEDGMENTS

The work reported in this paper was carried out with support from the Defense Advanced Research Projects Agency–University Research Initiative Consortium administered by the Office of Naval Research (under Contract No. N00014-86-K-0760), U.S. Department of Defense. The work at Purdue University and at the University of Notre Dame also received support from the National Science Foundation, Grants No. DMR-89-21717 and No. DMR-89-13706, respectively.

[1]N. Samarth, H. Luo, J. K. Furdyna, R. G. Alonso, Y. R. Lee, A. K. Ramdas, S. B. Qadri, and N. Otsuka, Appl. Phys. Lett. **56**, 1163 (1990).

[2]J. K. Furdyna, J. Appl. Phys. **64**, R29 (1988).

[3]J. K. Furdyna, J. Kossut, and A. K. Ramdas, in *Optical Properties of Narrow-Gap Low-Dimensional Structures,* edited by C. M. Sotomayor-Torres (Plenum, New York, 1987), p. 135.

[4]See R. L. Gunshor, L. A. Kolodziejski, A. V. Nurmikko, and N. Otsuka, in *Strained-Layer Superlattices: Materials Science and Technology,* edited by T. P. Pearsall, Semiconductors and Semimetals Vol. 33, edited by R. K. Willardson and A. C. Beer (Academic, New York, 1991), p. 337.

[5]E.-K. Suh, D. U. Bartholomew, A. K. Ramdas, S. Rodriguez, S. Venugopalan, L. A. Kolodziejski, and R. L. Gunshor, Phys. Rev. B **36**, 4316 (1987).

[6]R. G. Alonso, Eunsoon Oh, A. K. Ramdas, H. Luo, N. Samarth, J. K. Furdyna, and L. R. Ram-Mohan, Phys. Rev. B **44**, 8009 (1991).

[7]R. G. Alonso, E. -K. Suh, A. K. Ramdas, N. Samarth, H. Luo, and J. K. Furdyna, Phys. Rev. B **40**, 3720 (1989).

[8]R. G. Alonso, Y. R. Lee, Eunsoon Oh, A. K. Ramdas, H. Luo, N. Samarth, J. K. Furdyna, and H. Pascher, Phys. Rev. B **43**, 9610 (1991).

[9](a) H. Jeon, J. Ding, A. V. Nurmikko, H. Luo, N. Samarth, J. K. Furdyna, W. A. Bonner, and R. E. Nahory, Appl. Phys. Lett. **57**, 2413 (1990); (b) J. Ding, H. Jeon, A. V. Nurmikko, H. Luo, N. Samarth, and J. K. Furdyna, *ibid.* **57**, 2756 (1990); (c) J. Ding, N. Pelekanos, A. V. Nurmikko, H. Luo, N. Samarth, and J. K. Furdyna, *ibid.* **57**, 2885 (1990).

[10]Y. R. Lee, A. K. Ramdas, F. A. Chambers, J. M. Meese, and L. R. Ram-Mohan, Appl. Phys. Lett. **50**, 600 (1987).

[11]Y. R. Lee, A. K. Ramdas, A. L. Moretti, F. A. Chambers, G. P. Devane, and L. R. Ram-Mohan, Phys. Rev. B **41**, 8380 (1990).

[12]C. Parks, R. G. Alonso, A. K. Ramdas, H. Luo, N. Samarth, J. K. Furdyna, and L. R. Ram-Mohan, Bull. Am. Phys. Soc.

36, 861 (1991).

[13]M. Cardona, *Modulation Spectroscopy Solid State Physics,* Suppl. 11 of *Solid State Physics,* edited by F. Seitz, D. Turnbull, and H. Ehrenreich (Academic, New York, 1969), p. 89.

[14]Stainless-steel cryostat model "Super-Tran VP" and "Super Varitemp" Model 10DT, Janis Research, Inc., P.O. Box 696, 2 Jewel Ave., Wilmington, MA 01887-0896.

[15]B. O. Seraphin and N. Bottka, Phys. Rev. **145**, 628 (1966).

[16]M. Okuyama, T. Nishino, and Y. Hamakawa, J. Phys. Soc. Jpn. **35**, 134 (1973).

[17]D. E. Aspnes, Phys. Rev. Lett. **28**, 168 (1972).

[18]P. C. Klipstein and N. Apsley, J. Phys. C **19**, 6461 (1986).

[19]H. Luo, G. L. Yang, J. K. Furdyna, and L. R. Ram-Mohan, J. Vac. Sci. Technol. B **9**, 1809 (1991).

[20]W. J. Walecki, A. V. Nurmikko, N. Samarth, H. Luo, J. K. Furdyna, and N. Otsuka, Appl. Phys. Lett. **57**, 466 (1990).

[21]L. R. Ram-Mohan, K. H. Yoo, and R. L. Aggarwal, Phys. Rev. B **38**, 6151 (1988).

[22]K. H. Yoo, L. R. Ram-Mohan, and D. F. Nelson, Phys. Rev. B **39**, 12 808 (1989).

[23]M. H. Weiler, in *Semiconductors and Semimetals,* edited by R. K. Willardson and A. C. Beer (Academic, New York, 1981), Vol. 16, p. 119.

[24]See Eq. (4.9) in A. K. Ramdas and S. Rodriguez, in *Progress in Electron Properties of Solids,* edited by R. Girlanda *et al.* (Kluwer Academic, Amsterdam, 1989), pp. 65–98. See also G. L. Bir and G. E. Pikus, *Symmetry and Strain-induced Effects in Semiconductors* (Wiley, New York, 1974). Note: the curly brackets denote an anticommutator.

[25]H. J. Lozykowski and V. K. Shastri, J. Appl. Phys. **69**, 3235 (1991).

[26]A. S. Barker, Jr. and R. Loudon, Rev. Mod. Phys. **44**, 18 (1972).